Low-field magnetoresponse of strongly disordered two-dimensional superconductors

S. Sankar and V. Tripathi

Department of Theoretical Physics, Tata Institute of Fundamental Research, Homi Bhabha Road, Navy Nagar, Mumbai 400005, India

(Received 26 April 2016; revised manuscript received 25 July 2016; published 29 August 2016)

Weak magnetic fields significantly affect the properties of strongly disordered superconductors through diamagnetic orbital shrinking as well as geometric phase frustration effects. The relative importance of these orbital effects is analyzed for thin films in physical regimes dominated by a Coulomb blockade, thermal phase fluctuations, and phase frustration, respectively, using phenomenological and replica field theory approaches. As an important outcome, we obtain the field dependences of superfluid stiffness and resistance, and we show that they can be used to distinguish between phase frustration and diamagnetic shrinking effects. We also find that even though highly disordered films may never become superconducting, their inhomogeneous structure leaves a distinct signature on the magnetoresistance. The predicted low-field magnetoresistance is in very good accord with experiment.

DOI: 10.1103/PhysRevB.94.054520

I. INTRODUCTION

One of the most challenging problems in strongly disordered superconductors relates to understanding the nature of the magnetic-field-induced superconductor-normal state transition (SNT). Experimental and theoretical studies over the past two decades have led to a large number of puzzling questions, such as determining the origin of the giant nonmonotonous magnetic-field dependence of the resistivity [1–7], flux quantization in the insulating state [8], and the universality class governing the field-induced SNT [3,9–11]. The two-dimensional (2D) case in particular has attracted intense theoretical attention, and it is the focus of this work. In the absence of a magnetic field, it is well known that strong homogeneous disorder introduces granularity in the form of superconducting islands embedded in an insulating matrix [12–16]. However, the relative importance of diamagnetic (orbital) shrinking effects [4,5] and phase frustration effects brought about by the Aharonov-Bohm (AB) phases of the Cooper pairs tunneling across the islands [17,18] is not well understood.

Mean-field analyses of the field sensitivity of the distribution of superconducting regions go back nearly two decades for weakly disordered metals [19,20], and more recently [4] for strongly disordered insulators. Standard, perturbative approaches fail in the strongly disordered regime, but numerical mean-field solutions of the appropriate Bogoliubov–de Gennes (BdG) equations [4], reveal a picture of shrinking superconducting regions in increasing fields and a downward shift of the distribution of the local superconducting gaps. Then through the Ambegaokar-Baratoff relation [21], a corresponding decrease in the Josephson couplings J between neighboring grains is deduced. For fields much smaller than the pair breaking value, the dominant contribution to the field dependence of J comes from orbital shrinking effects. To understand the physical origin of these effects, we study a phenomenological model of repulsive bosons (Cooper pairs) subjected to a disordered potential and a perpendicular magnetic field. The approach is reminiscent of earlier work on Lifshitz states [22] in disordered Bose systems [5,23,24].

We show that orbital shrinking in the presence of a magnetic field suppresses the Josephson couplings as $J(B) \sim \exp[-(B/B_J)^2]$, and it is a primary cause of the strong magnetoresponse seen in experiments.

To understand the magnetoresponse of these 2D granular superconductors, we study the standard Josephson-junction (XY) model,

$$L = \frac{1}{4E_c}\sum_{\mathbf{i}}(\partial_\tau \phi_{\mathbf{i}})^2 - \sum_{\langle \mathbf{ij}\rangle} J_{\mathbf{ij}}(B)\cos(\phi_{\mathbf{ij}} + A_{\mathbf{ij}}), \quad (1)$$

where E_c represents the Coulomb-blockade scale, $\phi_{\mathbf{ij}} = \phi_{\mathbf{i}} - \phi_{\mathbf{j}}$ is the superconducting phase difference between neighboring grains at positions $\mathbf{i}$ and $\mathbf{j}$, respectively, and $A_{\mathbf{ij}} = (2e/\hbar)\int_{\mathbf{i}}^{\mathbf{j}} \mathbf{A}\cdot d\mathbf{r}$ are the AB phases acquired by the hopping Cooper pairs. Disregarding the contribution of normal quasiparticles means the model can provide a good description of the magnetoresponse only at lower fields where Cooper pair breaking is not important. Spatial disorder in the grain positions introduces randomness in the Josephson couplings as well as the AB phases. Studies of the 2D classical limit of Eq. (1) in the $B = 0$ limit [4] have shown that strong disorder in J does not alter the universality class of the SNT from the homogeneous case [where it is known to be of Kosterlitz-Thouless (KT) type], but it is nevertheless dominated by a percolating backbone of paths with the largest local superfluid stiffnesses. Likewise, the transition in the quantum 1D disordered counterpart at $B = 0$ also obeys a KT-like scaling [25–28]. Therefore, for simplicity we will work with the typical value of J, ignoring its spatial disorder.

In regular lattices, the AB phase is associated with flux threading the plaquettes, and depending on the amount of frustration f (measured as a fraction of a flux quantum), it leads to oscillations in properties such as the critical current and the resistance [29,30]. Such matching (commensuration) effects are absent in the disordered case as there is random flux penetration in different plaquettes. Phase transition in the classical quenched random-phase XY model on a square lattice close to integer f is well studied [31–34]. The presence of disorder results in rare favorable regions for the occurrence of vortices at low temperatures. At sufficiently low temperatures [32–34], it is found that the disorder-induced phase transition is not in the KT universality class. Very similar results were also obtained earlier [26] in a study

of the Anderson localization in one-dimensional Luttinger liquids subjected to quenched phase disorder. The similarity is puzzling since quenched disorder in one dimension is equivalent to columnar disorder in the two-dimensional case. Quantum Monte Carlo studies [18] of the interplay of phase frustration and Coulomb blockade suggest a zero-temperature field-driven SNT with dynamic exponent $z \approx 1.3$, placing the transition in a different universality class from 3D XY.

In this paper, we study the effect of three dominant mechanisms governing the loss of phase coherence and their specific signatures on the magnetoresistance and superfluid stiffness. These are (a) quantum phase fluctuations originating from a Coulomb blockade, (b) thermal fluctuations of the phase, and (c) frustration effects due to disorder in AB phases. We show that Coulomb-blockade effects impart a specific signature to the magnetoresistance, $\rho(B) \sim \exp[(B/B_0)^2]$. Where the SNT is driven by thermal fluctuations, we find a KT transition, with $\rho(B) \sim \exp[-1/\sqrt{B - B_{\rm KT}}]$ in the critical region. In the AB phase frustration dominated regime, we find a new, non-KT critical behavior, $\rho(B) \sim \exp[-1/(B - B_{AB})]$. The field-dependent superfluid stiffness Υ also shows a surprising behavior: at small fields, we predict that phase frustration effects on Υ are more significant than the field dependence of Josephson couplings. In the Coulomb-blockade regime away from the critical region, our predicted magnetoresistance is in excellent accord with experimental data [1,2]. However, in the critical scaling region, existing experimental data are somewhat less clear, and while there is some evidence for mechanism (c) for the field-tuned SNT in oxide heterostructures [35], further study is needed, and we propose additional probes to distinguish between the two.

The rest of the paper is organized as follows. Section II contains an analysis of the effect of a transverse magnetic field on the distribution of Cooper pairs in the presence of strong disorder. This analysis provides parameters for the effective Josephson junction model [Eq. (1)]. Three regimes of interest corresponding to different limits of parameters in the effective Josephson junction model are analyzed in Sec. III. Explicit expressions for the low-field magnetoresistance and superfluid stiffness are obtained here. Section IV compares these results with experiment, which is followed by a discussion in Sec. V.

II. DISORDERED BOSON MODEL

In this section, we analyze the effect of a transverse magnetic field on the distribution of Cooper pair islands in the granular superconductor, and we use this to estimate parameters in the effective Josephson junction model of Eq. (1). Consider a model of repulsive bosons (Cooper pairs) with average density n subjected to a random potential with a Gaussian white noise distribution:

$$H = \sum_{\mathbf{p}} \frac{\Pi^2}{2m} a^\dagger_{\mathbf{p}} a_{\mathbf{p}} + \int_{\mathbf{r}} \left[\frac{g}{2} |\Psi(\mathbf{r})|^4 + U(\mathbf{r}) |\Psi(\mathbf{r})|^2 \right], \quad (2)$$

where $\Psi(\mathbf{r}) = \frac{1}{\sqrt{V}} \sum_{\mathbf{p}} a_{\mathbf{p}} \exp[i\mathbf{p}\cdot\mathbf{r}/\hbar], \Pi = (\mathbf{p} - q\mathbf{A})$, $U(\mathbf{r})$ is the random potential, $\langle U(\mathbf{r})\rangle = 0$, $\langle U(\mathbf{r})U(\mathbf{r}')\rangle = \kappa^2 \delta(\mathbf{r} - \mathbf{r}')$, $q = 2e$ is the boson charge, and g parametrizes the boson repulsion. We choose the gauge $\mathbf{A} = \frac{1}{2}(\mathbf{B} \times \mathbf{r})$ with the field in the transverse z direction. This model is equivalent to the previously studied (for $B = 0$) Ginzburg-Landau models with disorder in critical temperature [12]. The important length scales in the model are the single-particle localization length $\mathcal{L} = \hbar^2/m\kappa$ characterizing the disorder, and the magnetic length $l_B = \sqrt{\hbar c/(eB)}$. At finite temperatures, the model has at least three parameters: $\gamma_1 = \mathcal{L}/l_B$, $\gamma_2 = 2mg/\hbar^2$, and $\gamma_3 = \mathcal{L}/\lambda_T$, where λ_T is the de Broglie wavelength. We are specifically interested in the regime where all three parameters are small. At low densities, the interplay of disorder and interparticle repulsion leads to the formation of disconnected islands of localized bosons [24] whose typical size and separation may be estimated as follows. The optimal potential fluctuation that has a bound state at energy $E < 0$ is found by minimizing $\frac{1}{2}\int U^2 d\mathbf{r} + \lambda(E - H)$, where λ is a Lagrange multiplier. We choose Ψ to be real, assuming a spherical fluctuation and a zero angular momentum bound state. Varying with respect to U, we obtain $U = \lambda\Psi^2$; thus the size R of the optimum potential well is also of the same order as the wave function. The energy of a particle in an island, in the mean-field approximation, is thus of the order of

$$E \sim -\frac{\hbar^2}{2mR^2} + \frac{(qBR)^2}{8m} + gN_p/(\pi R^2), \quad (3)$$

where N_p is the number of bosons in the island. The density $n_w = n/N_p$ of these islands is determined by the Gaussian factor, $\exp[-\frac{1}{2\kappa^2}\int_{\mathbf{r}} U^2]$, from which

$$n_w \sim \left(\frac{1}{\pi R^2}\right) \exp[-(\mathcal{L}/R)^2]. \quad (4)$$

Minimizing the energy with respect to R, the size of the typical island, to logarithmic precision, is

$$R(B) \sim \frac{\mathcal{L}}{\sqrt{\ln[n_c(B)/n]}}, \quad (5)$$

where for small fields,

$$n_c(B) \approx \frac{\hbar^2}{2gm\mathcal{L}^2}\left(1 + \frac{(qB\mathcal{L}^2/\hbar)^2}{4}\frac{1}{\ln^2[n_c(0)/n]}\right) \quad (6)$$

is the critical density for percolation of the islands, and $n_c(B)/n > 1$. For future convenience, we introduce $w(B) = n_c(B)/n$. Clearly, the magnetic field shrinks the islands, but the field dependence is very different from a simple expectation from wave-function shrinking of a localized noninteracting particle. The distance $D \sim 1/\sqrt{n_w}$ between the islands can be estimated as

$$D(B) \sim R(B)e^{\frac{1}{2}[\mathcal{L}/R(B)]^2} \sim \mathcal{L}\frac{\sqrt{w(B)}}{\sqrt{\ln w(B)}}. \quad (7)$$

The strength of tunneling of the bosons across the nearest islands can be estimated from the semiclassical formula $t = \exp(-1/\hbar\int |p| dl)$, where the integral path connects the two wells. The integral can be estimated using $|p| \sim \sqrt{2m|E|} \sim \hbar/R(B)$ and the length of the path is $\sim D(B)$. This leads to $t \sim \exp[-D(B)/R(B)]$. The Josephson coupling between the

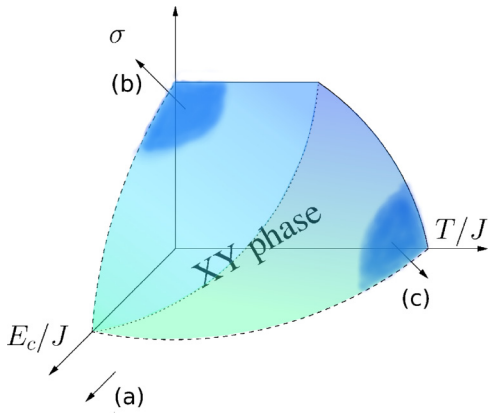

FIG. 1. Schematic phase diagram for the 2D superconductor-normal state transition, with the XY superfluid phase in the interior of the surface, as a function of dimensionless temperature T/J, Coulomb-blockade scale E_c/J, and the Aharanov-Bohm (AB) phase disorder σ for the model described in Eq. (1). Here J is the (field-dependent) Josephson coupling estimated in the paper. Part (a) illustrates the Coulomb-blockade-dominated regime. The shaded regions (b) and (c) denote transitions driven by AB phase frustration and thermal phase fluctuation, respectively. The dotted line on the surface separates these two different critical scaling regimes. The critical disorder at low T and E_c is independent of T, and the scaling of the correlation length is not of Kosterlitz-Thouless type [34].

nearest islands is $J \propto t^2$. Thus we obtain

$$J(B) \sim e^{-2\sqrt{w(B)}}. \tag{8}$$

Note that even when at small magnetic fields $\mathcal{L}/l_B \ll 1$, the exponent in Eq. (8) can be large at low boson densities, $w(B) \gg 1$. For such fields, we have $J(B)/J(0) \sim e^{-(B/B_J)^2}$, where $B_J^{-2} \approx \frac{\sqrt{w(0)}}{\ln^2 w(0)}(q\mathcal{L}^2/2\hbar)^2$.

Even though the value of R is fixed in our mean-field analysis, D and J nevertheless fluctuate since the wells have a finite probability density n_w to appear in any part of the system. It is straightforward to show that the distance D between neighboring grains has the distribution

$$P(D) \sim (2\pi D n_w) e^{-n_w \pi D^2}. \tag{9}$$

We now analyze the effects of the three different mechanisms that lead to a loss of global phase coherence in their regimes of dominance, which are determined by the dimensionless parameters E_c/J, T/J, and σ, with the latter a measure of disorder in the fluxes through elementary plaquettes. Figure 1 shows the phase diagram and the regimes of our study. To carry out this analysis, it is convenient to work with an effective Hamiltonian that has only the collective phases of different grains as the degrees of freedom. It is well known that our system can be described by a Josephson junction model with the Hamiltonian corresponding to the Lagrangian in (1). The magnetic-field-dependent parameters of the Hamiltonian are obtained from our analysis above. $E_c(B) = q^2/2C$ is the typical charging energy of the grains, where C is the typical capacitance of the grains; $C \sim \epsilon R(B)$, ϵ being the dielectric constant. Denoting the plaquette area fluctuation by $(\delta D)^2$, we identify $\sigma \sim B^2(\delta D)^4$. From Eq. (9), it follows that $(\delta D)/D \lesssim 1$.

III. ANALYSIS OF THE EFFECTIVE JOSEPHSON JUNCTION MODEL

We now proceed to the analysis of the effective Josephson junction model in the three different regimes mentioned above.

A. Quantum phase fluctuation dominated insulating regime ($E_c/J, E_c/T \gg 1$)

We treat the Josephson term in Eq. (1) as a perturbation, and we calculate the conductivity using the Kubo formula [36,37]. Transport in this model proceeds through Arrhenius activation and incoherent sequential hopping of charges between neighboring islands—this leads to a resistivity of the form

$$\rho(B) \sim J(B)^{-2} e^{E_c(B)/T} \sim e^{[4\sqrt{w(B)} + (q^2/\mathcal{L}T)\sqrt{\ln w(B)}]}. \tag{10}$$

The above behavior shows the insulating nature of the normal state. For small fields, the magnetoresistance obeys the law $\rho(B)/\rho(0) \sim \exp[(B/B_0)^2]$, where $B_0^{-2} \approx \frac{(q\mathcal{L}^2/2\hbar)^2}{2\ln^2 w(0)}[\sqrt{w(0)} + \frac{q^2}{\mathcal{L}T\sqrt{\ln w(0)}}]$. More accurately, one must also take into account the renormalization of the charging energy by Josephson coupling [37,38], $E_c \to E_c - J$. It is interesting to note that a similar field dependence of resistivity, $\rho(B) \sim e^{(B/B_c - 1)^2}$, has been obtained in the context of a superconductor to Hall insulator transition [39].

B. AB phase frustration dominated regime ($E_c/J \ll 1, T/J \ll 1, \sigma/\sigma_c \sim 1$)

To study this regime, it is useful to consider the Coulomb gas representation of the model in Eq. (1). Following earlier works [34,40], we assume a Gaussian white noise distribution for the AB phases on the links, reckoned from a background average corresponding to a typical separation of islands, D. In the Coulomb gas representation, such disorder translates to a random flux threading elementary plaquettes, corresponding to an external potential $V_{\mathbf{r}}$ acting on the "charges" (vortices) with a Gaussian distribution $\langle (V_{\mathbf{r}} - V_{\mathbf{r}'})^2 \rangle = 4\sigma J^2 \ln|\mathbf{r} - \mathbf{r}'| + O(1)$. It is crucial that the random background potential has long-range (logarithmic) correlations. In the continuum description of the model with a lower cutoff scale a_0, $V_{\mathbf{r}}$ has a local part, $v_{\mathbf{r}} : \langle (v_{\mathbf{r}} - v_{\mathbf{r}'})^2 \rangle \sim \sigma J^2$, and a long-range correlated part, $V_{\mathbf{r}}^{>}$, with no cross-correlation between these two parts. The Coulomb gas Hamiltonian then reads

$$H = -J \sum_{\mathbf{r} \neq \mathbf{r}'} n_{\mathbf{r}} n_{\mathbf{r}'} \ln\left(\frac{|\mathbf{r} - \mathbf{r}'|}{a_0}\right) - \sum_{\mathbf{r}} [n_{\mathbf{r}} V_{\mathbf{r}}^{>} - \ln Y[n_{\mathbf{r}}, \mathbf{r}]], \tag{11}$$

where $n_{\mathbf{r}}$ represents the integer charge at $\mathbf{r}$, the spatially dependent fugacities have the bare value $\ln Y[n_{\mathbf{r}}, \mathbf{r}] = \gamma J n_{\mathbf{r}}^2 + n_{\mathbf{r}} v_{\mathbf{r}}$, and γ is a constant of order unity. We have dropped the background term as it just sets the chemical potential of the vortices and does not affect the scaling equations [41].

In the absence of disorder, the usual RG procedure consists of (i) increasing the short-scale cutoff, $a_0 \to a_0 + dl$, and eliminating all dipoles in the annulus of thickness dl, and (ii) disregarding all configurations that increase the net charge within the cutoff region. The RG procedure is perturbatively

controlled by small dipole fugacities. For the disordered case, we follow Ref. [34] and introduce replicas, which allows us to perform the average over Gaussian disorder. The lowest excitations continue to carry charges $0, \pm 1$, but now the $n_{\mathbf{r}}^{\alpha}$ also carry a replica index α. An important difference from the RG procedure of the disorder-free case is that now when the cutoff is increased, one must, apart from considering annihilation of replica charges, also take into account "fusion" of unit charges in different replicas (see the Appendix A). Another important difference that invalidates the usual perturbative expansion in small dipole fugacities is that the random potential creates favorable regions for single vortex formation. Hence we study the scale dependence of the single vortex fugacity distribution identifying the density of rare favorable regions, $\rho_{a_0}^{v}$, for the occurrence of vortices as the perturbation parameter. By studying the scaling of $\rho_{a_0}^{v}$, two distinct regimes can be identified for $T/J \ll 1$: (a) an XY phase at sufficiently low bare disorder, where $\rho_{a_0}^{v}$ scales to zero, and (b) a disordered phase beyond a critical bare disorder where $\rho_{a_0}^{v}$ diverges (see the Appendix B for details). In the disordered phase, the phase correlation length has a surprising non-KT behavior, $\xi \sim e^{1/(\sigma-\sigma_c)}$, which in our context translates to a field dependence $\xi \sim e^{1/(B-B_{\mathrm{AB}})}$, with $B_{\mathrm{AB}} \sim \hbar/q(\delta D)^2$. Such a non-KT behavior is a direct consequence of the logarithmic scaling of the disorder potential correlations. Another peculiarity is that over a range of low temperatures up to a scale of order J, the critical disorder σ_c is independent of the temperature [34].

We obtain the magnetic-field dependence of the superfluid stiffness by solving the scaling equations in the critical region at low temperatures for the coupling constant J_l and the effective disorder σ_l. Taking the ratio of the scaling equations for J_l and σ_l obtained in Ref. [34], we get

$$\frac{\partial_l J_l^{-1}}{\partial_l \sigma_l} \sim \frac{1}{J_l \sqrt{\sigma_l}},$$

and from the solution $J_l \sim e^{-2\sqrt{\sigma_l}}$ it follows that the superfluid stiffness $\Upsilon(B)$ has the behavior

$$\Upsilon(B) \sim J(B) e^{-2\sqrt{\sigma(B)}} \sim e^{-(B/B_1)-(B/B_J)^2}, \qquad (12)$$

where B_1 is of the order of B_{AB}. Phase frustration effects thus play a more important role in determining the low-field dependence of superfluid stiffness in the AB phase frustration dominated regime compared to the effect coming from orbital shrinking.

Now we analyze magnetoresistance in the disordered phase at low temperatures and close to the field-induced transition. Following Halperin and Nelson [42], we estimate the electrical resistivity (which is essentially the vortex conductivity) as $\rho(B) = \mu_v n(B)$, where μ_v is the temperature and field-dependent mobility of the vortices, and $n(B) \sim 1/\xi^2$ is the vortex density. We make an assumption that $\mu_v(B)$ is well-behaved near $B = B_{\mathrm{AB}}$, which allows us to neglect its field dependence in comparison to the singular behavior of $\xi(B)$. The temperature dependence of resistivity is governed by the temperature dependence of the mobility, and we believe it shows an activated behavior given the logarithmic Coulomb interaction of the vortices [43]. The magnetoresistance in this AB phase frustration dominated regime thus grows as

$$\rho(B) \sim \mu_v(T) e^{-1/(B-B_{\mathrm{AB}})}. \qquad (13)$$

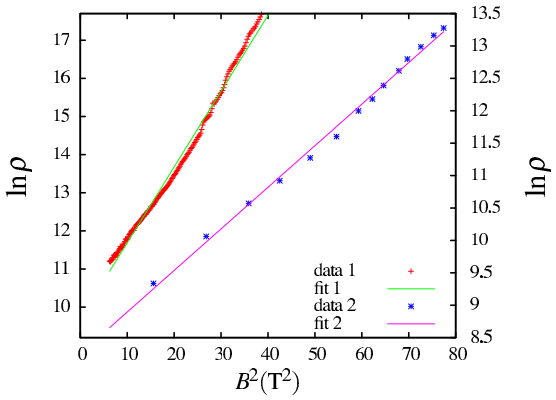

FIG. 2. Resistivity ρ as a function of perpendicular magnetic field B for disordered InO_x thin films as reported in Ref. [1] (data 1) and Ref. [2] (data 2) in the low-field region where the fits are to the predicted behavior $\rho(B) \sim e^{(B/B_0)^2}$ corresponding to the Coulomb-blockade-dominated regime discussed in the text.

C. Thermal phase fluctuation dominated KT regime $[E_c/J \ll 1, \sigma/\sigma_c \ll 1, T/J(B) \sim 1]$

In this regime, the transition is brought about by the proliferation of thermally activated vortices. The superfluid stiffness now has a field dependence $\Upsilon(B) \sim J(B) \sim e^{-(B/B_J)^2}$ arising from orbital shrinking of the superconducting islands. For the resistivity, we again consider the correlation length in the disordered phase, which has the well-known form $\xi \sim e^{1/\sqrt{T-T_{KT}}}$, with $T_{\mathrm{KT}} \propto J(B)$. Near the transition, this is equivalent to a field-dependent correlation length, $\xi \sim e^{1/\sqrt{B-B_{\mathrm{KT}}}}$. Thus the resistivity in this regime has the form

$$\rho(B) \sim \mu_v(T) e^{-1/\sqrt{B-B_{\mathrm{KT}}}}. \qquad (14)$$

For regimes (b) and (c), the normal state has a "metallic" temperature dependence since enhancement of vortex mobilities at higher temperatures translates to higher resistivity.

IV. RELATION TO EXPERIMENTS

Figure 2 shows the low-temperature and low-field magnetoresistance of disordered InO_x thin films extracted from two different experiments [1,2]. The positive magnetoresistance data are very well-described by Eq. (10), which places these samples in our Coulomb-blockade-dominated regime. Deviation from the Coulomb-blockade prediction is seen near the magnetoresistance peak, and we believe this is due to the quasiparticle transport channel opening up. In samples with lower disorder [2], unsurprisingly, the Coulomb blockade does not adequately explain the data; however, the other critical scaling regimes (AB phase frustration and KT) show better agreement, even though we were unable to distinguish between the two (see the Appendix B). In a recent study of the field-tuned SNT at 2D interfaces of gated oxide heterostructures [35], it was reported that for certain gate voltages, the critical magnetic field at low temperatures was independent of the temperature, suggestive of the phase frustration driven SNT mechanism. Finally, our predictions for superfluid stiffness in the XY regime can possibly be tested through studies of field-dependent ac conductivity [44], and they may provide an

independent means for distinguishing between the two regimes in the XY phase.

V. DISCUSSION

In summary, we studied the field dependence of the distribution of SC islands in strongly disordered superconductors, and we constructed an effective Josephson-junction model with field-dependent parameters. Analyzing the model in different physical regimes—dominated by a Coulomb blockade, thermal phase fluctuations, or Aharanov-Bohm phase fluctuations—we obtained the field dependence of resistivity and superfluid stiffness. In the Coulomb-blockade regime, available experimental data are in excellent agreement with our prediction $\rho(B) \sim e^{(B/B_0)^2}$, while in the critical scaling region, available magnetoresistance data [2] are insufficient to distinguish between KT and AB phase frustration regimes.

At very low temperatures, the critical behavior in the vicinity of the quantum critical point $[E_c/J(B) \sim 1]$ is expected to be that of the 3D XY universality class. For the field-tuned transition in systems with homogeneous potential disorder, the rapid decrease of the Josephson coupling $J(B)$ with field implies that the likely experimental trajectories in the T/J versus E_c/J plane rapidly move out of the quantum critical region into the Coulomb-blockade-dominated region where $E_c/J \gg 1$. In contrast, in systems such as nanopatterned superconducting proximity arrays, the fabrication technique is such that the separation of superconducting regions [and thus $J(B)$] is not as field-sensitive. Such systems look attractive from the point of view of studying the critical behavior near the field-tuned SNT, especially in the quantum critical region $E_c/J(B) \sim 1$. In our study, we neglected pair-breaking effects, which likely play a crucial role in explaining the giant negative magnetoresistance observed at higher fields [4,5]. Pair breaking opens up an additional quasiparticle transport channel, and it would be interesting to study magnetic-field effects in phase models with both quasiparticle and Cooper pair tunneling.

ACKNOWLEDGMENTS

We are grateful to G. Sambandamurthy for sharing his experimental data with us, and to Y. Meir, P. Raychaudhuri, and E. Shimshoni for valuable discussions, and V. Vinokur for his critical reading of the paper and discussions. V.T. thanks Department of Science and Technology, India, for a Swarnajayanti grant (DST/SJF/PSA-0212012-13), and Argonne National Laboratory, where a significant part of this work was completed.

APPENDIX A: RG EQUATIONS AND THE PHASE DIAGRAM OF THE DISORDERED XY MODEL

In this Appendix, we show the essential steps followed to obtain the phase diagram of the two-dimensional XY model with phase disorder. A comprehensive study can be found in Ref. [34].

The partition function of the replicated Coulomb gas with *m-vector* charges after averaging over the bare disorder is

$$\overline{Z^m} = 1 + \sum_{p=2}^{\infty} \sum_{\mathbf{n}_1,\ldots,\mathbf{n}_p} \int_{|\mathbf{r}_i - \mathbf{r}_j| > a_0} \exp(-\beta H^{(m)}[\mathbf{n},\mathbf{r}]),$$

where the sum is over all distinct neutral configurations, and

$$\beta H^{(m)} = \sum_{i \neq j} K_{ab} n_i^a \ln\left(\frac{|\mathbf{r}_i - \mathbf{r}_j|}{a_0}\right) n_j^b + \sum_i \ln Y[\mathbf{n}_i].$$

Here, $Y[\mathbf{n}] = \exp(-n^a \gamma K_{ab} n^b)$, where $K_{ab} = \beta J \delta_{ab} - \sigma \beta^2 J^2$. Significant contribution to the partition function only comes from charges $\pm 1,0$, and hence we restrict to these. We increase the hard-core cutoff $a_0 \to a_0 e^{(dl)}$ and retain the original form of the partition function in terms of scale-dependent coupling constants $(K_l)_{ab}$ and fugacities $Y_l[\mathbf{n}]$. To $O(Y[\mathbf{n}]^2)$, we obtain the following RG flow equations [34]:

$$\partial_l \left(K_l^{-1}\right)_{ab} = 2\pi^2 \sum_{\mathbf{n} \neq \mathbf{0}} n^a n^b Y[\mathbf{n}] Y[-\mathbf{n}], \tag{A1}$$

$$\partial_l Y[\mathbf{n} \neq \mathbf{0}] = (2 - n^a K_{ab} n^b) Y[\mathbf{n}] + \sum_{\mathbf{n}' \neq 0, \mathbf{n}} \pi Y[\mathbf{n}'] Y[\mathbf{n} - \mathbf{n}']. \tag{A2}$$

Equation (A1) comes from the annihilation of dipoles of opposite vector charges in the annulus $a_0 < |r_i - r_j| < a_0 e^{dl}$. It gives the renormalization of the interaction and of the disorder. Simple rescaling gives the first part of Eq. (A2). The second part comes from the possibility of fusion of two replica vector charges upon coarse-graining. Some examples of fusion are given below,

$$\begin{pmatrix} \vdots \\ +1 \\ \vdots \\ +1 \\ \vdots \\ 0 \\ \vdots \end{pmatrix} + \begin{pmatrix} \vdots \\ 0 \\ \vdots \\ 0 \\ \vdots \\ -1 \\ \vdots \end{pmatrix} \to \begin{pmatrix} \vdots \\ +1 \\ \vdots \\ +1 \\ \vdots \\ -1 \\ \vdots \end{pmatrix}, \quad \begin{pmatrix} \vdots \\ +1 \\ \vdots \\ 0 \\ \vdots \\ 0 \\ \vdots \end{pmatrix} + \begin{pmatrix} \vdots \\ 0 \\ \vdots \\ +1 \\ \vdots \\ 0 \\ \vdots \end{pmatrix} \to \begin{pmatrix} \vdots \\ +1 \\ \vdots \\ +1 \\ \vdots \\ 0 \\ \vdots \end{pmatrix}, \quad \begin{pmatrix} \vdots \\ +1 \\ \vdots \\ 0 \\ \vdots \\ +1 \\ \vdots \end{pmatrix} + \begin{pmatrix} \vdots \\ -1 \\ \vdots \\ 0 \\ \vdots \\ 0 \\ \vdots \end{pmatrix} \to \begin{pmatrix} \vdots \\ 0 \\ \vdots \\ 0 \\ \vdots \\ +1 \\ \vdots \end{pmatrix}.$$

Replica permutation symmetry, which we will assume here and which is preserved by the RG, together with $n^a = 0, \pm 1$, implies that $Y[\mathbf{n}]$ depends only on the numbers n_+ and n_- of $+1/-1$ components of $\mathbf{n}$. We parametrize $Y[\mathbf{n}]$ by introducing

a function of two arguments $\Phi(z_+,z_-)$, where $z_\pm(\mathbf{r}) = \exp(\pm\beta v_\mathbf{r})$, such that

$$Y[\mathbf{n}] = \langle z_+^{n_+} z_-^{n_-}\rangle_\Phi, \tag{A3}$$

where we denote $\langle A\rangle_\Phi = \int dz_+ dz_- A\Phi(z_+,z_-)$. After some manipulations [34], in the limit $m \to 0$, we can write Eq. (A2) in terms of $P = \phi/(\int_{z_+,z_->0}\phi)$, which can be interpreted as a probability distribution, as

$$\begin{aligned}\partial_l P(z_+,z_-) &= OP - 2P(z_+,z_-) + 2\left\langle \delta\left(z_+ - \frac{z_+^{'} + z_+^{''}}{1 + z_-^{'}z_+^{''} + z_+^{'}z_-^{''}}\right)\right.\\ &\left.\times\,\delta\left(z_- - \frac{z_-^{'} + z_-^{''}}{1 + z_-^{'}z_+^{''} + z_+^{'}z_-^{''}}\right)\right\rangle_{P'P''},\end{aligned} \tag{A4}$$

where $O = \beta J(2 + z_+\partial_{z_+} + z_-\partial_{z_-}) + \sigma(\beta J)^2(z_+\partial_{z_+} - z_-\partial_{z_-})^2$. The $m \to 0$ limit of Eq. (A1) similarly yields

$$T\frac{dJ^{-1}}{dl} = 8\left\langle \frac{z_+^{'}z_-^{''} + z_-^{'}z_+^{''} + 4z_+^{'}z_-^{''}z_-^{'}z_+^{''}}{(1 + z_+^{'}z_-^{''} + z_-^{'}z_+^{''})^2}\right\rangle_{PP}, \tag{A5}$$

$$\frac{d\sigma}{dl} = 8\left\langle \frac{(z_+^{'}z_-^{''} - z_-^{'}z_+^{''})^2}{(1 + z_+^{'}z_-^{''} + z_-^{'}z_+^{''})^2}\right\rangle_{PP}. \tag{A6}$$

Equations (A4), (A5), and (A6) form the complete set of RG equations.

Numerical study [34] of the RG equations indicates the existence of an XY phase at low temperatures and below some critical disorder. Guided by the RG flow observed numerically within and near the boundaries of the XY phase, we can approximate the full RG equations using a simpler equation involving only the single fugacity distribution, $P_l(z) = \int dz_+ P_l(z_+,z) = \int dz_- P_l(z,z_-)$. In the low-$T$ regime, the distribution $P_l(z_+,z_-)$ is broad and the physics is dominated by rare favorable regions ($z_+ \sim 1$ or $z_- \sim 1$). Here we identify a parameter that allows us to organize perturbation theory as follows: $P_l(1) \equiv P_l(z \sim 1) \sim P_l(z_+ \sim 1, z_- \sim 0) = P_l(z_+ \sim 0, z_- \sim 1)$. We also observe that $P_l(1,1) \equiv P_l(z_+ \sim 1, z_- \sim 1) \sim P_l(1)^2$. Using these, we can see schematically the RG equation (A4) as a correction to $P_l(1)$ of order $P_l(1)$ by the first term and order $P_l(1)^2$ by the second term; and in RG equations (A5) and (A6) as a correction to order $P_l(1)^2$ to J_l and σ_l. Again working to order $P_l(1)^2$, we see that the denominators in the δ functions in (A4) could be neglected. This approximation also simplifies Eqs. (A5) and (A6).

Introducing

$$G_l(x) = 1 - \int_{-\infty}^{\infty} du\, \tilde{P}_l(u)\exp(-e^{\beta(u-x+E_l)}), \tag{A7}$$

where $u = 1/\beta\ln(z)$ and $E_l = \int_0^l J(l^{'})dl^{'}$, we see that (A4) can be written as $\frac{1}{2}\partial_l G = \frac{\sigma J^2}{2}\partial_x^2 G + G(1-G)$. If σ and J are l-independent, we identify the above with Kolmogorov-Petrovskii-Piscounov (KPP) equation, whose general form is $\frac{1}{2}\partial_l G = D\partial_x^2 G + f(G)$, where D is a constant and f satisfies $f(0) = f(1) = 0$, f is positive between 0 and 1, and $f^{'}(0) = 1, f^{'}(G) \leqslant 1$ between 0 and 1. Since at large l, both J and σ converge and effectively become l-independent, we see that we can use results from the study of the KPP equation in our case at large l.

For a large class of initial conditions, the solutions of the KPP equation are known to converge uniformly toward traveling wave solutions of the form $G_l(x) \to h(x - m_l)$. The velocity of the wave is given by $c = \lim_{l\to\infty}\partial_l m_l$. A theorem due to Bramson [45] shows that the asymptotic traveling wave is determined by the behavior at $x \to \infty$ of the initial condition $G_{l=0}(x)$ in the following manner. If $G_{l=0}(x)$ decays faster than $e^{-\mu x}$, where $\mu = 1/\sqrt{D}$, then $c = \sqrt{D}$. If $G_{l=0}(x)$ decays slower than $e^{-\mu x}$, where $\mu < 1/\sqrt{D}$, then $c = 2(D\mu + \mu^{-1})$. The parametrization (A7) implies that the distribution $\tilde{P}_l(u)$ itself converges to a traveling front solution

$$\tilde{P}_l(u) \to_{l\to\infty} \tilde{p}(u - X_l), \quad X_l = m_l - E_l. \tag{A8}$$

Since $\partial_l E_l \to_{l\to\infty} J_R$, we see that the asymptotic velocity of the front of $\tilde{P}_l(u)$ is $c - J_R$, where c is the KPP front velocity. The center of the front corresponds to the maximum of the distribution $\tilde{P}(u)$.

The asymptotic velocity clearly decides the phase of the system: since we start with a distribution peaked at some small z, if the velocity is positive, then $P_l(1)$ will increase, and this would imply that the system is in the disordered phase. On the other hand, negative velocity implies that the system is in the XY phase. The velocity vanishes at the phase boundary. By construction, the initial condition $G_{l=0}(x)$ decays for large x as $\langle z\rangle_{P_0} e^{-\beta x}$. Hence we identify $\mu = \beta$. Based on the results discussed above about the front velocity selection in the KPP equation, we can conclude the following about the phase diagram of the model:

(a) For $T > T_g = J_R\sqrt{\sigma_R/2}$, $c = T(2 + \frac{\sigma_R J_R^2}{T^2})$. Thus here the XY phase would exist for

$$2 - \frac{J_R}{T} + \frac{\sigma_R J_R^2}{T^2} < 0. \tag{A9}$$

(b) For $T \leqslant T_g$, $c = J_R\sqrt{8\sigma_R}$. Thus here the XY phase would exist for $\sigma_R < \sigma_c = \frac{1}{8}$.

Critical behavior at zero temperature: The zero-temperature phase transition from the XY phase to the disordered phase occurs at $\sigma_R = 1/8$. The center of the front is located at $u = X_l$ near the transition. It follows from [45] that $X_l \approx (4\sqrt{D} - J)l - 3/2\sqrt{D}\ln l + X_0$. Hence in the critical region to leading order, we get

$$\partial_l X_l \sim 4\sqrt{D} - J - \frac{3\sqrt{D}}{2l}. \tag{A10}$$

After some manipulations, the RG equations for J and σ in the critical region read

$$\partial_l(J^{-1}) = k\int du\, \tilde{p}_l(u - X_l)\tilde{p}_l(-u - X_l),$$

$$\partial_l\sigma = k\int_{u+u^{'}>-2X_l} \tilde{p}_l(u)\tilde{p}_l(u^{'}),$$

where k is some constant. Using the asymptotic form of $\tilde{p}_l(u)$ discussed in [45] and working up to leading order in $(\sigma - \sigma_c)$,

we can simplify the above equations to obtain

$$\partial_l(J^{-1}) \sim \frac{C}{\sqrt{D}} X_l^3 \exp\left(\frac{2X_l}{\sqrt{D}}\right),$$

$$\partial_l \sigma \sim C X_l^3 \exp\left(\frac{2X_l}{\sqrt{D}}\right),$$

where C is a constant. To estimate the form of correlation length, we first introduce the small parameter, $g_l = \exp(X_l/\sqrt{D})$. Then (A10) reads

$$\partial_l g \sim \left(16(\sigma - \sigma_c) - \frac{3}{2l}\right) g.$$

Now starting away from criticality, $\epsilon = \sigma_c - \sigma_R > 0$, we find $g_l \sim l^{-3/2} \exp(16\epsilon l)$. Identifying the correlation length ξ as when $g_\xi \sim 1$, we find

$$\xi \sim \exp\left(\frac{b}{|\sigma - \sigma_c|}\right),$$

where b is some constant. We then see that the universality class of this transition is clearly different from the KT universality class.

APPENDIX B: COMPARISON OF KOSTERLITZ-THOULESS (KT) AND NON-KT SCALING WITH EXPERIMENTS

In Fig. 3, we show the sheet resistance $R_\square$ versus magnetic-field data near a field-driven SIT in a homogeneously disordered InO_x thin film from Ref. [2], and we attempt to fit these data to the Kosterlitz-Thouless (KT) behavior ($R_\square = R_0 e^{-1/\sqrt{B-B_{KT}}}$) and the non-KT behavior ($R_\square = R_0 e^{-1/(B-B_{AB})}$) obtained in this paper. It is difficult to say which of these two laws describes the data better; however, we argue that the non-KT fit might be a bit better on account of a more reasonable value for the high-field resistance R_0.

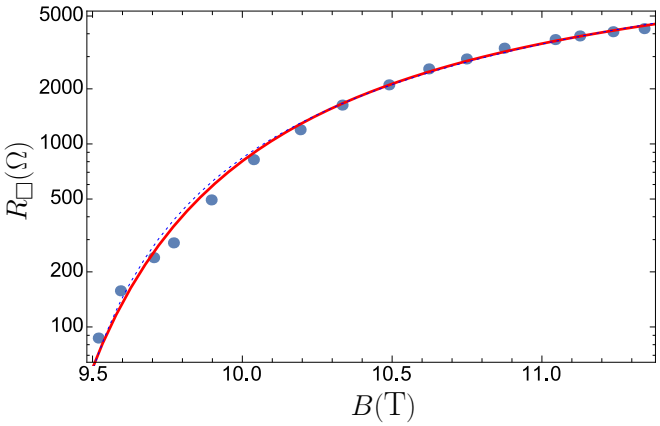

FIG. 3. Sheet resistance $R_\square$ of homogeneously disordered InO_x thin films as a function of perpendicular magnetic field B near the field-driven SIT (data extracted from Ref. [2]). The fits are to a Kosterlitz-Thouless (KT) law $R_\square = 5.02\times10^4 e^{-16/\sqrt{B^2-9.22^2}}$ (solid red curve) and the non-KT law $R_\square = 1.53\times10^4 e^{-61.2/(B^2-8.9^2)}$ (blue dashed curve). The KT transition is driven by thermal phase fluctuations, while the non-KT transition is driven by phase frustration. Both laws fit the data equally well; however, the prefactor of the exponential, which represents the high-field sheet resistance, is a more reasonable number in the non-KT case since in the actual data, the peak value of resistance is of comparable order.

[1] G. Sambandamurthy, L. W. Engel, A. Johansson, and D. Shahar, Phys. Rev. Lett. **92**, 107005 (2004).
[2] M. A. Steiner, G. Boebinger, and A. Kapitulnik, Phys. Rev. Lett. **94**, 107008 (2005).
[3] E. L. Shangina and V. T. Dolgopolov, Phys. Usp. **46**, 777 (2003).
[4] Y. Dubi, Y. Meir, and Y. Avishai, Phys. Rev. B **73**, 054509 (2006).
[5] V. L. Pokrovsky, G. M. Falco, and T. Nattermann, Phys. Rev. Lett. **105**, 267001 (2010).
[6] V. M. Galitski, G. Refael, M. P. A. Fisher, and T. Senthil, Phys. Rev. Lett. **95**, 077002 (2005).
[7] A. V. Lopatin and V. M. Vinokur, Phys. Rev. B **75**, 092201 (2007).
[8] M. Stewart, A. Yin, J. Xu, and J. M. Valles, Science **318**, 1273 (2007).
[9] N. P. Breznay, M. A. Steiner, S. A. Kivelson, and A. Kapitulnik, Proc. Natl. Acad. Sci. USA **113**, 280 (2016).
[10] M. A. Paalanen, A. F. Hebard, and R. R. Ruel, Phys. Rev. Lett. **69**, 1604 (1992).
[11] M. P. A. Fisher, Phys. Rev. Lett. **65**, 923 (1990).
[12] L. B. Ioffe and A. I. Larkin, Sov. Phys.-JETP **54**(2), 378 (1981).
[13] M. P. A. Fisher, P. B. Weichman, G. Grinstein, and D. S. Fisher, Phys. Rev. B **40**, 546 (1989).
[14] A. Ghosal, M. Randeria, and N. Trivedi, Phys. Rev. Lett. **81**, 3940 (1998).
[15] B. Sacépé, C. Chapelier, T. I. Baturina, V. M. Vinokur, M. R. Baklanov, and M. Sanquer, Phys. Rev. Lett. **101**, 157006 (2008).
[16] M. Chand, G. Saraswat, A. Kamlapure, M. Mondal, S. Kumar, J. Jesudasan, V. Bagwe, L. Benfatto, V. Tripathi, and P. Raychaudhuri, Phys. Rev. B **85**, 014508 (2012).
[17] A. Chakrabarti and C. Dasgupta, Phys. Rev. B **37**, 7557 (1988).
[18] K. Kim and D. Stroud, Phys. Rev. B **78**, 174517 (2008).
[19] B. Spivak and F. Zhou, Phys. Rev. Lett. **74**, 2800 (1995).
[20] V. M. Galitski and A. I. Larkin, Phys. Rev. Lett. **87**, 087001 (2001).
[21] V. Ambegaokar and A. Baratoff, Phys. Rev. Lett. **10**, 486 (1963).
[22] I. Lifshitz, Sov. Phys. JETP **26**, 462 (1968).
[23] A. I. Larkin and V. M. Vinokur, Phys. Rev. Lett. **75**, 4666 (1995).
[24] G. M. Falco, T. Nattermann, and V. L. Pokrovsky, Phys. Rev. B **80**, 104515 (2009).
[25] E. Altman, Y. Kafri, A. Polkovnikov, and G. Refael, Phys. Rev. Lett. **93**, 150402 (2004).
[26] T. Giamarchi and H. J. Schulz, Phys. Rev. B **37**, 325 (1988).
[27] E. Altman, Y. Kafri, A. Polkovnikov, and G. Refael, Phys. Rev. Lett. **100**, 170402 (2008).
[28] F. Hrahsheh and T. Vojta, Phys. Rev. Lett. **109**, 265303 (2012).
[29] S. Teitel and C. Jayaprakash, Phys. Rev. Lett. **51**, 1999 (1983).

[30] H. S. J. van der Zant, W. J. Elion, L. J. Geerligs, and J. E. Mooij, Phys. Rev. B **54**, 10081 (1996).
[31] M.-C. Cha and H. A. Fertig, Phys. Rev. Lett. **74**, 4867 (1995).
[32] T. Nattermann, S. Scheidl, S. E. Korshunov, and M. S. Li, J. Phys. I **5**, 565 (1995).
[33] D. Carpentier and P. Le Doussal, Phys. Rev. Lett. **81**, 2558 (1998).
[34] D. Carpentier and P. Le Doussal, Nucl. Phys. B **588**, 565 (2000).
[35] J. Biscaras, N. Bergeal, S. Hurand, C. Feuillet-Palma, A. Rastogi, R. Budhani, M. Grilli, S. Caprara, and J. Lesueur, Nat. Mater. **12**, 542 (2013).
[36] V. Tripathi and Y. L. Loh, Phys. Rev. Lett. **96**, 046805 (2006).
[37] S. V. Syzranov, K. B. Efetov, and B. L. Altshuler, Phys. Rev. Lett. **103**, 127001 (2009).
[38] M. V. Fistul, V. M. Vinokur, and T. I. Baturina, Phys. Rev. Lett. **100**, 086805 (2008).
[39] E. Shimshoni, A. Auerbach, and A. Kapitulnik, Phys. Rev. Lett. **80**, 3352 (1998).
[40] A. Petković, V. M. Vinokur, and T. Nattermann, Phys. Rev. B **80**, 212504 (2009).
[41] V. Oganesyan, D. A. Huse, and S. L. Sondhi, Phys. Rev. B **73**, 094503 (2006).
[42] B. Halperin and D. R. Nelson, J. Low Temp. Phys. **36**, 599 (1979).
[43] B. I. Shklovskii, arXiv:0803.3331.
[44] S. Misra, L. Urban, M. Kim, G. Sambandamurthy, and A. Yazdani, Phys. Rev. Lett. **110**, 037002 (2013).
[45] M. Bramson, Mem. Am. Math. Soc. **44**, 1 (1983).